



EUROPEAN
HEMATOLOGY
ASSOCIATION



Ferrata Storti
Foundation

Factor VIII/V C-domain swaps reveal discrete C-domain roles in factor VIII function and intracellular trafficking

Eduard H.T.M. Ebberink,^{1*} Eveline A.M. Bouwens,^{1*} Esther Bloem,¹ Mariëtte Boon-Spijker,¹ Maartje van den Biggelaar,¹ Jan Voorberg,^{1,3} Alexander B. Meijer^{1,2} and Koen Mertens^{1,2}

¹Department of Plasma Proteins, Sanquin Research, Amsterdam; ²Department of Pharmaceutics, Utrecht Institute for Pharmaceutical Sciences, Utrecht University and ³Landsteiner Laboratory of AMC and Sanquin, University of Amsterdam, the Netherlands

*EHTM and EAMB contributed equally to this work

Haematologica 2017
Volume 102(4):686-694

ABSTRACT

Factor VIII C-domains are believed to have specific functions in cofactor activity and in interactions with von Willebrand factor. We have previously shown that factor VIII is co-targeted with von Willebrand factor to the Weibel-Palade bodies in blood outgrowth endothelial cells, even when factor VIII carries mutations in the light chain that are associated with defective von Willebrand factor binding. In this study, we addressed the contribution of individual factor VIII C-domains in intracellular targeting, von Willebrand factor binding and cofactor activity by factor VIII/V C-domain swapping. Blood outgrowth endothelial cells were transduced with lentivirus encoding factor V, factor VIII or YFP-tagged C-domain chimeras, and examined by confocal microscopy. The same chimeras were produced in HEK293-cells for *in vitro* characterization and chemical foot-printing by mass spectrometry. In contrast to factor VIII, factor V did not target to Weibel-Palade bodies. The chimeras showed reduced Weibel-Palade body targeting, suggesting that this requires the factor VIII C1-C2 region. The factor VIII/V-C1 chimera did not bind von Willebrand factor and had reduced affinity for activated factor IX, whereas the factor VIII/V-C2 chimera showed a minor reduction in von Willebrand factor binding and normal interaction with activated factor IX. This suggests that mainly the C1-domain carries factor VIII-specific features in assembly with von Willebrand factor and activated factor IX. Foot-printing analysis of the chimeras revealed increased exposure of lysine residues in the A1/C2- and C1/C2-domain interface, suggesting increased C2-domain mobility and disruption of the natural C-domain tandem pair orientation. Apparently, this affects intracellular trafficking, but not extracellular function.

Correspondence:

k.mertens@sanquin.nl

Received: August 2, 2016.

Accepted: December 23, 2016.

Pre-published: January 5, 2017.

doi:10.3324/haematol.2016.153163

Check the online version for the most updated information on this article, online supplements, and information on authorship & disclosures: www.haematologica.org/content/102/4/686

©2017 Ferrata Storti Foundation

Material published in *Haematologica* is covered by copyright. All rights are reserved to the Ferrata Storti Foundation. Use of published material is allowed under the following terms and conditions:

<https://creativecommons.org/licenses/by-nc/4.0/legalcode>.

Copies of published material are allowed for personal or internal use. Sharing published material for non-commercial purposes is subject to the following conditions:

<https://creativecommons.org/licenses/by-nc/4.0/legalcode>,

sect. 3. Reproducing and sharing published material for commercial purposes is not allowed without permission in writing from the publisher.



Introduction

Factor VIII (FVIII) serves as a co-factor for activated factor IX (FIXa) in the factor X (FX) activating complex. It consists of 2332 amino acids with a distinct domain structure: A1-a1-A2-a2-B-a3-A3-C1-C2.¹ Intracellular processing of the B-domain yields a heterodimeric FVIII protein with a 90-220 kDa heavy chain (A1-a1-A2-a2) non-covalently associated with a 80 kDa light chain (a3-A3-C1-C2).² FVIII circulates in complex with the multimeric glycoprotein von Willebrand factor (VWF) that protects FVIII from premature clearance and proteolytic degradation. Complex assembly occurs over an extended surface on FVIII, spanning the entire light chain.³⁻⁵ The sulfated tyrosine on position 1680 is essential for binding to VWF and mutation of this tyrosine results in impaired complex formation with VWF.³

Recently it has been shown that FVIII is expressed in endothelial cells.⁶⁻⁸ Previous work showed that FVIII overexpressed in endothelial cells co-sorts with VWF to the

secretory organelles designated Weibel-Palade bodies (WPB).^{9,11} The precise interaction mediating sorting to WPB has not been clarified, although it has been generally assumed that VWF plays a key role as a sorting chaperone. In contrast to this view, we have shown that FVIII sorting to WPB does not require the high-affinity interaction via the sulfated tyrosine on position 1680 in the $\alpha 3$ -domain.^{11,12} Moreover, endothelial cells with mutations in the FVIII C1- and C2-domains leading to impaired extracellular VWF/FVIII complex assembly show apparently normal expression of FVIII and storage in WPB.¹²

Like FVIII, coagulation factor V (FV) comprises two lipid-binding C-domains that form a similar side-by-side pair.¹³⁻¹⁷ FV shares ~40% sequence homology with FVIII and has a similar domain structure (A1-A2- $\alpha 2$ -B-A3- $\alpha 3$ -C1-C2).¹⁸ FV functions as a cofactor for FXa in the prothrombinase complex, demonstrating that FVIII and FV serve a similar cofactor function. Unlike FVIII, however, FV neither circulates in complex with VWF, nor does it act as a cofactor for FIXa in the activation of FX. In the present study, we addressed the contribution of C-domains to FVIII intracellular targeting and extracellular function by constructing FVIII chimeras carrying FV C1- or C2-domains and exploring the functional and structural implications of these C-domain swaps.

Methods

Factor VIII constructs

All constructs used in this study encoded B-domain-deleted FVIII (BDD-FVIII) variants in order to meet size restrictions in the lentiviral packaging system.¹⁰ For the same reason FV, too, was B-domain-deleted (BDD-FV).¹⁹ In BDD-FVIII-YFP, yellow fluorescent protein (YFP) replaced the B-domain, as described for its green fluorescent protein (GFP) equivalent elsewhere.^{10,11} Construction of plasmids encoding the YFP-tagged BDD-FVIII/FV chimeras is described in the *Online Supplementary Material*. For functional studies, BDD-FVIII-YFP and the chimeras were constructed in the pcDNA3.1 vector for production in HEK293 cells. To simplify nomenclature, the term BDD-FVIII is replaced by FVIII throughout this paper. Consequently, the BDD-FVIII-YFP chimeras containing the FV-C1 or -C2 domain are referred to as FVIII-YFP/FV-C1 and FVIII-YFP/FV-C2, respectively.

Immunofluorescence microscopy of lentiviral-transduced endothelial cells

The isolation of blood outgrowth endothelial cells (BOEC) and their subsequent transduction with lentivirus have been described previously.¹⁰ A detailed description of the antibody staining of BDD-FV and BDD-FVIII can be found in the *Online Supplementary Material*. Z-stacks (0.4- μ m intervals) were taken with confocal laser scanning microscopy using a Zeiss LSM510 equipped with Plan NeoFluar 63x/1.4 Oil objective (Carl Zeiss, Heidelberg, Germany). Images were processed with Zeiss LSM510 version 4.0 software and LSM image browser (Carl Zeiss, Heidelberg, Germany). Secretion of FVIII and FV was quantified by enzyme-linked immunosorbent assay (ELISA) as described previously, with the exception that the FV ELISA used the monoclonal anti-light chain antibody CLB-FV-4, and purified FV as a reference.^{12,19}

Purified factor VIII-yellow fluorescent protein variants

FVIII-YFP/FV chimeras and FVIII-YFP were produced in stable cell lines (HEK293) and purified by immunoaffinity chromatography using a monoclonal antibody (VK34) followed by anion

exchange chromatography (Q Sepharose FF, GE Healthcare, Uppsala, Sweden) as described in detail elsewhere.²⁰ Purified FVIII-YFP variants were homogeneous, and comprised a YFP-carrying heavy chain of approximately 110 kDa and an 80 kDa light chain (see *Online Supplementary Figure S1*). FVIII-YFP concentrations were determined by ELISA, employing the monoclonal anti-light chain antibody KM33 (anti-C1) or EL14 (anti-C2) for immobilization, and the anti-heavy chain antibody CLB-CAg-9 for detection.²¹ Normal human plasma served as the standard. FVIII activity was determined using a chromogenic assay (Chromogenix, Milan, Italy), and the activity/antigen ratios were 1.0 for FVIII-YFP, 0.9 for FVIII-YFP/FV-C2, and 0.4 for FVIII-YFP/FV-C1. In all functional studies FVIII concentrations were based on antigen concentrations, assuming that 1 U/mL corresponds to 0.3 nM.

Characterization of factor VIII-yellow fluorescent protein variants

Interactions of purified FVIII-YFP variants with recombinant full-length VWF¹¹ were assessed by surface plasmon resonance analysis using a BIAcore 3000 biosensor (Biacore AB, Uppsala, Sweden) as described previously.²¹ Details of the data analysis are provided in the *Online Supplementary Material*. Interactions of FVIII-YFP and the FVIII-YFP/FV chimeras with FIXa and phospholipids were inferred from FX activation studies, as described in detail elsewhere.²¹ Structural differences between FVIII-YFP, FV and the C-domain-swapped chimeras were probed by chemical foot-printing using lysine-reactive tandem-mass-tags (TMT) and mass spectrometry as described previously.²² A full description of the processing of labeled proteins into peptides and mass spectrometry analysis is given in the *Online Supplementary Material*.

Results

Differential intracellular accumulation of factor V compared to factor VIII

Because FV is structurally highly homologous to FVIII, we compared FVIII and FV with respect to WPB trafficking in BOEC expressing BDD-FVIII or BDD-FV via lentiviral transduction. Transduced BOEC secreted much larger amounts of FV (140 pmol/10⁶ cells/72 h) than FVIII (typically 1-5 pmol/10⁶ cells/72 h). Confocal microscopy revealed that, as expected, FVIII retained within the endothelial cells completely co-localized with VWF in WPB (Figure 1A). Consistent with co-localization, FVIII-containing WPB were round.^{10,23,24} In contrast, FV did not traffic to WPB (Figure 1B). The FV-transduced cells contained WPB which were negative for FV and retained their typical elongated morphology similar to those of the surrounding non-transduced cells. Instead, prominent background staining for FV could be detected in what might represent the endoplasmic reticulum (Figure 1B). Apparently, trafficking of FV is different from that of FVIII.

C-domains of factor VIII contribute to intracellular trafficking

To study the contribution of individual C-domains of the C-domain pair to FVIII sorting, we exchanged single FVIII C-domains for those of FV. Because of potential difficulties in staining these variants with antibodies directed at the FVIII light chain, we expressed YFP-tagged FVIII (FVIII-YFP) in this experiment. To this end BOEC were transduced with lentivirus encoding for FVIII-YFP and YFP-tagged FVIII variants with swapped C1- or C2-

domain (FVIII-YFP/FV-C1 and FVIII-YFP/FV-C2). FVIII-YFP/FV chimera production, as assessed by antigen levels in the conditioned medium, ranged between 0.03 – 0.3 pmol/10⁶ cells/72 h. The inherent variability in expression levels and transduction efficiency did not allow for quantification of the WPB-targeted fraction of the FVIII-YFP/FV chimeras. However, for transduced BOEC, trafficking could be studied by fluorescence microscopy. Confocal microscopy showed that YFP-tagged FVIII sorted exclusively to WPB (Figure 2A) and was retained in round WPB, similar to untagged FVIII (Figure 1A). This was to be expected because YFP tags as such do not affect FVIII trafficking to WPB.^{12,24} Substitution of the C1-domain resulted in total loss of co-localization of FVIII-YFP/FV-C1 with VWF in WPB (Figure 2B). Like FV, FVIII-YFP/FV-C1 was shown to accumulate intracellularly, without any apparent punctuated YFP signal as seen in Figure 2A (upper right side panels). The FVIII-YFP/FV-C2 variant displayed some residual sorting involving round WPB (Figure 2C). However, not all WPB were positive for YFP (see inset, Figure 2C), and a major part of the YFP signal was localized intracellularly, presumably in the endoplasmic reticulum. These results indicate that the C1-domain is the main driver of FVIII trafficking to WPB, although the C2-domain contributes to this process as well.

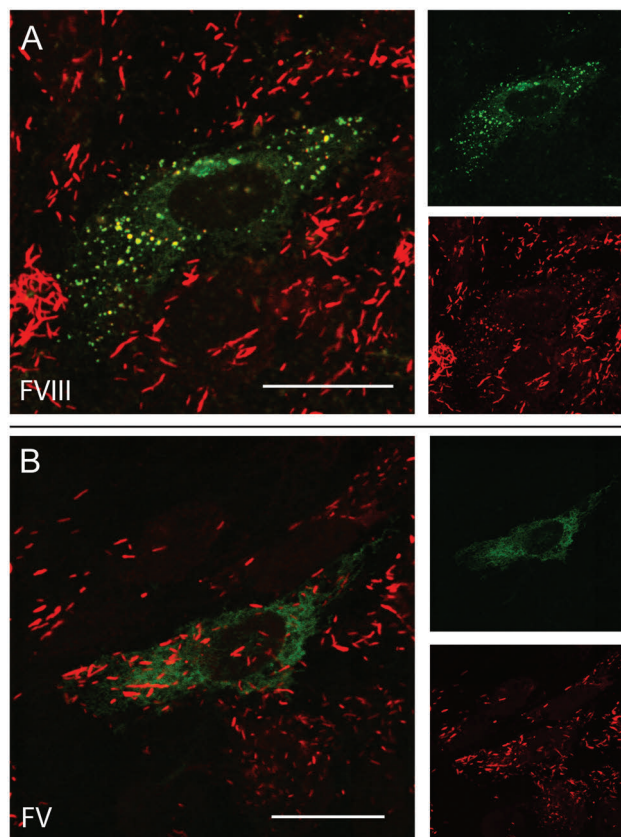


Figure 1. Differential sorting of FVIII and FV in blood outgrowth endothelial cells. Confocal images of BOEC expressing (A) B-domain-deleted FVIII or (B) B-domain-deleted FV. Both FVIII and FV are shown in green, and staining of VWF is shown in red. Yellow indicates co-localization of VWF with FVIII or FV. Images of the separate green and red channels are depicted on the right side. FVIII is solely visible co-stored with VWF in WPB. While FVIII-containing WPB have a round morphology, FVIII-negative WPB remain elongated. FV is not visible in WPB. The white scale bar represents 20 μ m.

The factor VIII C1-domain is critical for von Willebrand factor-binding

Given that the FVIII-YFP/FV chimeras displayed reduced co-localization with VWF in BOEC, we studied the ability of the chimeras to interact with VWF employing surface plasmon resonance analysis. This enables a time-resolved monitoring of the association and dissociation between two interactive proteins, by measuring mass increase and

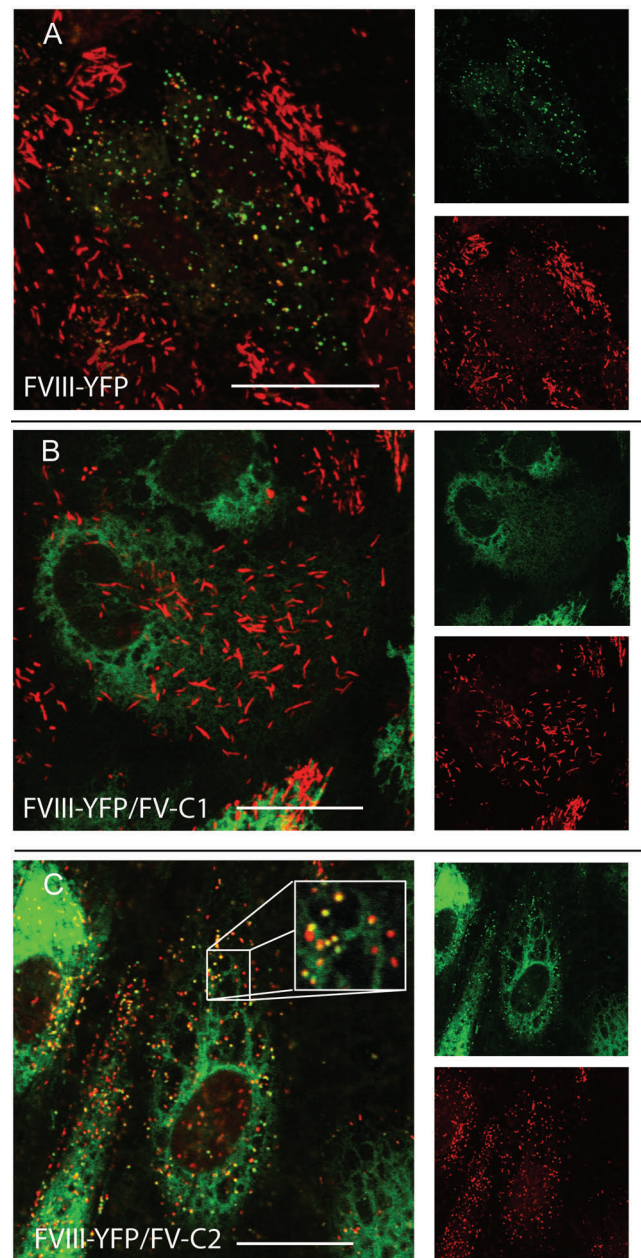


Figure 2. Intracellular localization of FVIII-YFP/FV-C1 and FVIII-YFP/FV-C2 chimeras in blood outgrowth endothelial cells. Confocal microscopy of BOEC expressing YFP-tagged B-domain-deleted FVIII variants. Merged signals of the YFP-tagged FVIII variants (green) and Alexa-633 stained VWF (red) (co-localization in yellow) are shown on the left side. On the right side image exports of the separate channels are displayed: YFP (green) top panel and Alexa-633 (red) lower panel. (A) YFP-tagged FVIII co-localizes with VWF in round WPB, while surrounding non-transduced BOEC, which are negative for YFP, contain elongated WPB. (B) FVIII-YFP/FV-C1 does not co-localize with VWF, and the WPB remain elongated. (C) Some of FVIII-YFP/FV-C2 is located in round WPB with VWF, but most of the FVIII-YFP/FV-C2 is dispersed throughout the cell. The white scale bar represents 20 μ m.

decrease due to the interaction of a soluble component (in this case, FVIII-YFP/FV chimeras) with an immobilized binding partner (in this case, VWF).^{12,21} FVIII-YFP variants, in varying concentrations, were passed over a chip with immobilized VWF and analyzed for surface-bound mass change, expressed in Resonance Units (RU). Figure 3 shows the maximal binding response as a function of the FVIII concentration, which can be used to derive an estimate of the dissociation constant K_d .^{21,25} The apparent K_d for FVIII-YFP was 8 nM, while FVIII-YFP/FV-C2 showed a slight reduction in VWF binding, with an apparent K_d of approximately 16 nM. In contrast, FVIII-YFP/FV-C1 showed no appreciable interaction with VWF at all (Figure 3A). Similar data were obtained at pH 5.5, which should resemble the pH in the mature secretory compartment.²⁶ FVIII variants revealed complex binding kinetics, from which the affinity could not be directly inferred by standard curve fitting of the sensorgrams, due to pronounced heterogeneity in the dissociation phase at pH 5.5 (Online Supplementary Figure S2). Data obtained at pH 7.4 were

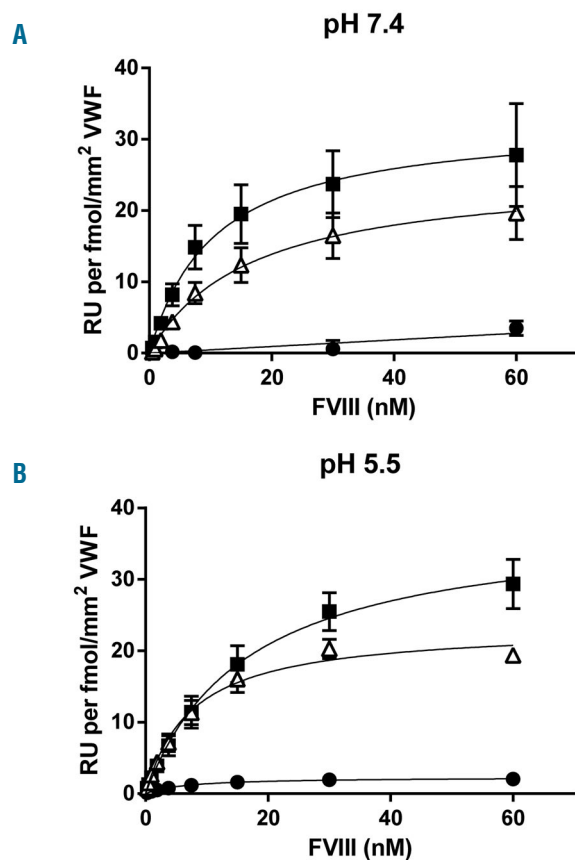


Figure 3. Interaction of FVIII-YFP and FVIII-YFP/FV chimeras with von Willebrand factor. Surface plasmon resonance (SPR) analysis was performed using the BIACore 3000 system as described elsewhere.²¹ FVIII-YFP (closed circles), FVIII-YFP/FV-C1 (closed circles) and FVIII-YFP/FV-C2 (open triangles) were passed over a CM5 chip coated with recombinant VWF (7, 24 and 37 fmol/mm²) in a buffer containing 150 mM NaCl, 5 mM CaCl₂, 2.4% glycerol (v/v), 0.005% Tween 20 (v/v), and 20 mM HEPES (pH 7.4, panel A) or 20 mM MES (pH 5.5, panel B) for 240 s at 20 μ L/min at 25 °C. The signal of a non-coated CM5 channel was subtracted to correct for differences in buffer composition. Response upon the onset of dissociation was taken to represent maximal binding and was plotted against the FVIII concentration. Values represent mean resonance units (RU) \pm SD. Data were analyzed by a non-linear regression using a single hyperbola. This revealed apparent K_d values of approximately 8 and 16 nM for FVIII-YFP and FVIII-YFP/FV-C2, respectively. VWF binding of FVIII-YFP/FV-C1 was too low for quantitative analysis. Individual SPR sensorgrams are shown in Online Supplementary Figure S2.

less complex, and revealed an apparent K_d of 3 nM for FVIII-YFP and 8 nM for FVIII-YFP/FV-C2. Irrespective of the data analysis used, these experiments demonstrate that FVIII-YFP/FV-C2 and FVIII-YFP display similar interactions with VWF, whereas FVIII-YFP/FV-C1 shows almost no VWF binding. Apparently, replacement of the FVIII C2-domain with that of FV conserves VWF-binding. In contrast, the FVIII C1-domain is irreplaceable for the interaction with VWF.

Substitution of the factor VIII C1-domain, but not C2-domain, affects cofactor activity

Thus far, purified chimeras were characterized in the absence of lipids although FVIII/FV C-domains are known to assemble on (negatively charged) membranes.¹³⁻¹⁶ To study the function of the FVIII-YFP/FV chimeras further, we examined complex formation with FIXa on phospholipid vesicles and their capability to convert the physiological substrate, FX. Membrane-binding was assessed by varying the phospholipid vesicle concentration at a fixed concentration of FIXa (16 nM). When using phospholipid vesicles containing 15% phosphatidylserine, no reduction in FXa generation rates were observed with FVIII-YFP/FV-C2 in comparison with FVIII-YFP (Figure 4A). A lower maximal FXa generation rate was seen with FVIII-YFP/FV-C1. However, both chimeras showed the same apparent affinity to membranes as FVIII-YFP (half-maximal response \sim 0.5 μ M). The reduction in maximal response of FVIII-YFP/FV-C1 is due to reduced binding of FIXa, as was assessed by varying the FIXa concentration at a fixed phospholipid concentration (Figure 4B). Therein, the FXa generation rates of FVIII-YFP/FV-C2 and FVIII-YFP are identical. FVIII-YFP/FV-C1, however, needed a concentration of at least 30 nM to reach the same level. Similar data were obtained in the presence of vesicles containing 5% phosphatidylserine, with the exception that the defect of the FVIII-YFP/FV-C1 variant proved more prominent (Figure 4D). At this low phosphatidylserine content the activity of FVIII-YFP/FV-C2 was also somewhat reduced at low lipid concentrations (Figure 4C). These data demonstrate that in terms of cofactor activity the C2-domain is interchangeable with that of FV. However, swapping the C1-domain introduces a defect that involves assembly with FIXa.

Distorted C-domain pairing in chimeras containing factor V C-domains

To examine the structural integrity of the chimeras, structural differences between FVIII-YFP and the chimeras were studied by lysine residue labeling with TMT. This approach consists of a pairwise comparison between proteins by labeling each with one of two isobaric labels (TMT-126 or TMT-127), which, upon tandem mass spectrometry, reveal their lysine-bound indicator mass of either 126 or 127 Da. This enables simultaneous identification and quantification of surface-exposed lysine residues.²² We used TMT-126 for FVIII-YFP and TMT-127 for the FVIII-YFP/FV chimeras and expressed relative incorporation of TMT labels in the ratio of TMT-127/TMT-126 per individual peptide. A ratio above 1 indicates increased lysine exposure in the FVIII-YFP/FV chimera (TMT-127 labeled) compared to the FVIII-YFP (TMT-126 labeled), and vice versa for ratios below 1.

Comparing the TMT-labeling incorporation of the FVIII-YFP/FV chimeras to that of FVIII-YFP revealed that for most of the lysine residues, TMT-127/TMT-126 ratios

were around 1 (*Online Supplementary Figure S3*). This indicates that accessibility for most of the lysine residues remained unchanged. However, some peptides showed a TMT-127/TMT-126 ratio >1 in both chimeras (*Figure 5A*). Most of these peptides contain lysine residues situated at the C2/A1-domain interface (Lys107, Lys123 and Lys127) (*Figure 5B*). Peptides covering the C2-domain lysine residues Lys2239 and Lys2249 showed increased accessibility only in FVIII-YFP/FV-C1 (*Figure 5A*). Due to the swapping of the C2-domain and thus the absence of TMT-127 labeled counterparts, FVIII-YFP/FV-C2 showed a TMT-127/TMT-126 ratio of almost zero for these lysine residues. Apart from lysine residues with increased accessibility, FVIII-YFP/FV-C2 also displayed lysine residues in the C1-domain with decreased accessibility. These are Lys2020, Lys2110 and/or Lys2111. (*Figure 5A, B and Online Supplementary Figure S3*).

Using TMT labeling, the lysine exposure of the swapped C-domains themselves could also be investigated in comparison with their native conformation in FV. This was done by labeling FV with TMT-126 and comparing it to the chimeras labeled with TMT-127. In this way only the swapped C-domains were examined. Again, most peptides displayed an unchanged lysine exposure (ratios were approximately 1). However, one C1-domain peptide containing two lysine residues directed towards the opposing C2-domain in the FV model had an average TMT-127/TMT-126 ratio of 3 (Lys1941 and Lys1954) (*Figure 6A,C*). Within the swapped C2-domain, two peptides indicated an increased accessibility of its lysine residues: one peptide with lysine residues directed towards to the C1-domain (Lys2157 and Lys2161) and one

peptide containing a lysine residue directed towards the A1-domain (Lys2137) (*Figure 6B,C*). Compared to FV, these lysine residues are more accessible for TMT labeling in the chimeras. Thus, taken together the comparisons between FVIII-YFP, FV and the chimeras, the C1/C2- and C2/A1-domain interfaces become exposed which suggests that pairing of the C-domains is altered in both FVIII-YFP/FV chimeras.

Discussion

The site of FVIII biosynthesis has remained a matter of debate. It was previously established that FVIII overexpression in BOEC leads to co-storage of FVIII with VWF in WPB.^{9,10} The relevance of this model system has recently been established by findings that FVIII is expressed in endothelial cells.⁶⁻⁸ However, the mechanism underlying FVIII trafficking and secretion remains poorly understood. Here we studied the expression of FVIII, FV and FVIII/FV C-domain chimeras in BOEC. In contrast to FV, FVIII was solely found in WPB (*Figure 1*). This implies a specific FVIII mechanism, which appears to be affected once one of the two FVIII C-domains is swapped with FV (*Figure 2*). Particularly, C1-domain swapping appeared destructive, although FVIII-YFP/FV-C2 also displayed a trafficking defect. Thus, both C-domains appear to contribute. Remarkably, C-domains that bind tightly to phospholipids tend to occur in a tandem pair as observed in FVIII, FV, lactadherin and developmental-endothelial-locus 1 (del-1).²⁷ Next to a tandem or multimeric organization, secretion of these strong lipid-binders tends to be regulated. For

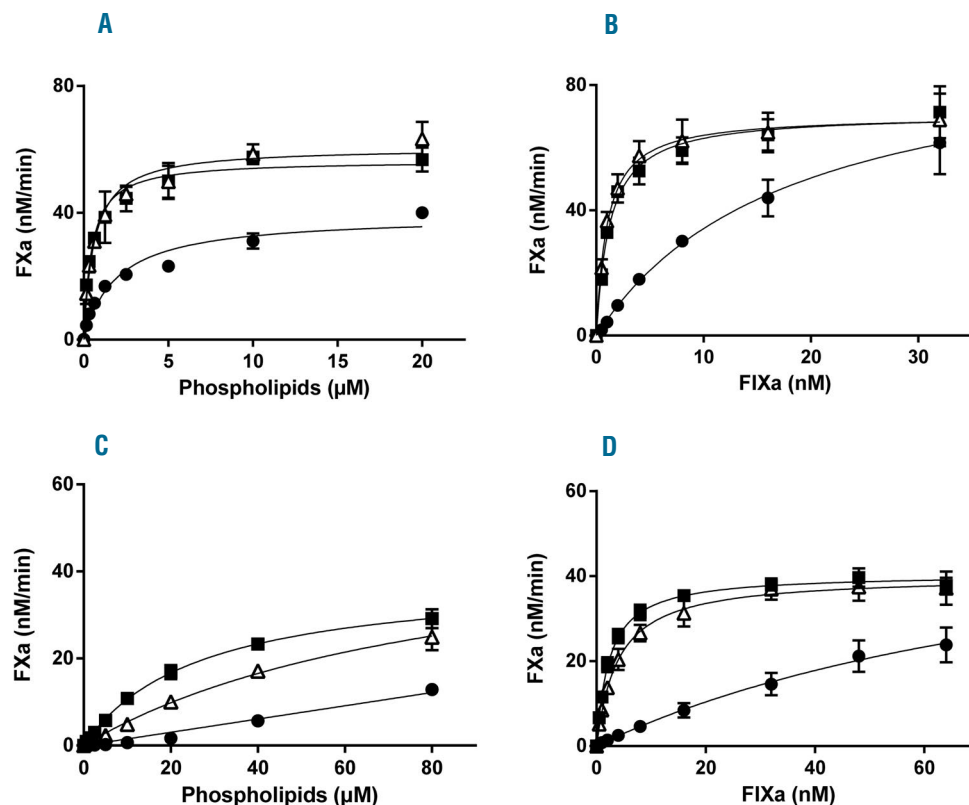


Figure 4. FVIII cofactor activity of the FVIII-YFP chimeras. FVIII-YFP (closed squares), FVIII-YFP/FV-C1 (closed circles) and FVIII-YFP/FV-C2 (open triangles) were examined for their capability to function as cofactor in the activation of FX. FX activation studies were performed in the presence of phospholipid vesicles containing 15% phosphatidylserine, 20% phosphatidylethanolamine, and 65% phosphatidylcholine (panels A and B) or 5% phosphatidylserine, 20% phosphatidylethanolamine, and 75% phosphatidylcholine panels (C and D) in a buffer containing 40 mM Tris-HCl (pH 7.8), 150 mM NaCl and 0.2% (w/v) bovine serum albumin. FXa titrations (panels B and D) were performed by incubation of 25 µM of phospholipid vesicles mixed with 0-64 nM FIXa, 0.3 nM FVIII and 200 nM FX. Phospholipid titrations (panels A and C) were performed by incubation of 0-80 µM phospholipid vesicles mixed with 16 nM FIXa, 0.3 nM FVIII and 200 nM FX. Reactions were initiated by addition of 1.5 mM CaCl₂ and 1 nM thrombin. Subsamples of the reaction mixture were taken at 30 s intervals and analyzed for FXa using the substrate S-2765 containing the thrombin inhibitor I-2581.²¹ Absorbance values were converted into molar concentrations using a standard curve of active-site titrated purified FXa.

instance, lactadherin released by several cell types is associated with confined membrane vesicles (exosomes).^{28,29} As reported by others, deletion of one of the two lactadherin C-domains results in a loss of the exosome-mediated secretion.²⁹ This suggests that trafficking of lactadherin requires an intact C-domain tandem pair, which might also be required for FVIII.

Within both FVIII-YFP/FV chimeras, TMT foot-printing revealed more accessibility between the A1/C2- and C1/C2-domain interface, implying a loose C-domain tandem pair with increased C2-domain mobility (Figures 5 and 6). This extends the notion that the C2-domain in FVIII has limited interdomain contacts.³⁰ In two available FVIII crystal structures,^{30,31} the C2-domain Lys2239 interaction with a nearby glutamic acid (Glu122 in the A1-domain) seems to be the only evident electrostatic interaction (*Online Supplementary Figure S4*). A swap of the C2-domain may affect this interaction even though Lys2293 is conserved in FV. The swapped Lys2239 could not be detected; however, Glu122 neighboring lysine residues

Lys123 and Lys127 could be measured and had an increased TMT-127/TMT-126 ratio (Figure 5). Strikingly, when swapping the C1-domain, Lys2239 could be resolved and also displayed increased labeling despite its remote location. Perhaps, introduction of a FV C-domain produces an unfavorable interaction in the C1/C2-domain interface which in turn affects the C2/A1-domain interface. By one-sided insertion of a FV C-domain in FVIII, interactions would be disrupted due to loss of the interacting counterparts. Indeed, Lys1941 and Lys2161 display increased accessibility in the chimeras while in FV they most likely interact with residues on their opposite C-domain Phe2163 and Glu2034 (*Online Supplementary Figure S4*).³² The A3/C1-domain interface could hardly be probed because it contains a limited number of lysine residues. Nonetheless three of these residues, at positions 2010, 2110 and 2111 in the C1-domain, displayed reduced surface exposure in the FVIII-YFP/FV-C2 chimera (Figure 5 and *Online Supplementary Figure S3*). The apparent protection of these lysine residues suggests that the top of the

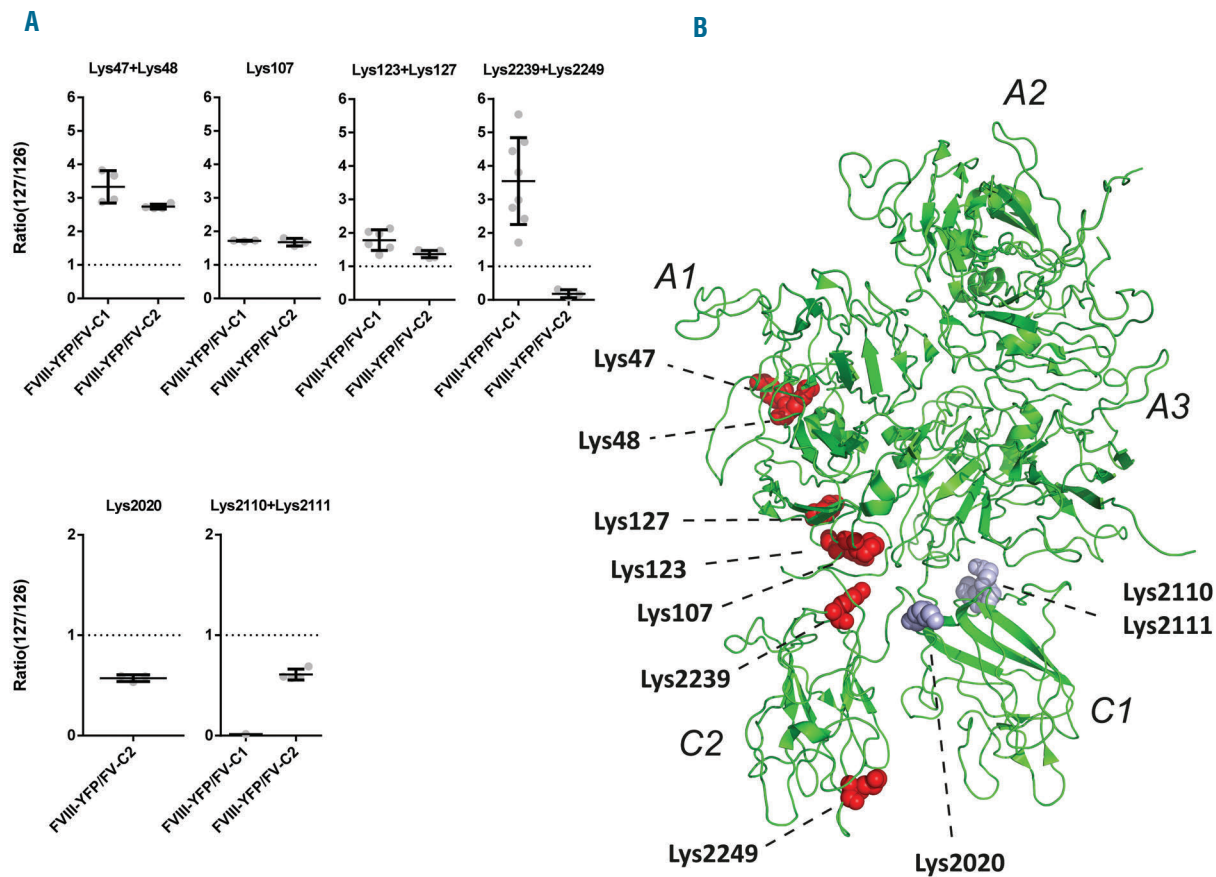


Figure 5. Comparison of FVIII-YFP/FV-C1 and FVIII-YFP/FV-C2 with FVIII-YFP by labeling with tandem-mass tags. FVIII-YFP/FV-C1 and FVIII-YFP/FV-C2 were labeled with TMT-127 and FVIII-YFP with TMT-126 to assess differences in lysine residue exposure. Labeled FVIII variants were then processed into peptides and measured for TMT incorporation. The lysine residues with a TMT-127/TMT-126 ratio different from 1 are: Lys47+Lys48, Lys107, Lys123+Lys127, Lys2020, Lys2110+Lys2111 and Lys2239+2249. (A) The peptides containing the same lysine residue(s) and their TMT-127/TMT-126 ratio per chimera are shown in the different panels. The mean TMT-127/TMT-126 ratio \pm SD is given by the black lines; peptides and their resolved TMT-127/TMT-126 ratio are represented by gray dots. A TMT-127/TMT-126 ratio above or below 1 (dashed line) indicates increased or decreased incorporation of TMT-127 and therefore altered accessibility of those lysine residues in the chimera compared to FVIII-YFP. Peptides covering lysine residues 2239 and 2249 show a TMT-127/TMT-126 ratio > 1 for chimera FVIII-YFP/FV-C1. In the FVIII-YFP/FV-C2 chimera these lysine residues have a near zero ratio because the FVIII C2-domain peptides are not present in the FVIII-YFP/FV-C2 chimera (only TMT-126 labeled FVIII-YFP lysine residues could be detected). Software analysis considers a TMT-127/TMT-126 ratio of zero erroneous and therefore may produce ratios with a minimum value of 0.01. (B) Lysine residues with increased accessibility for TMT labeling are indicated in the FVIII crystal structure (2R7E)³⁰ as red spheres, whereas lysine residues with reduced reactivity are indicated in blue.

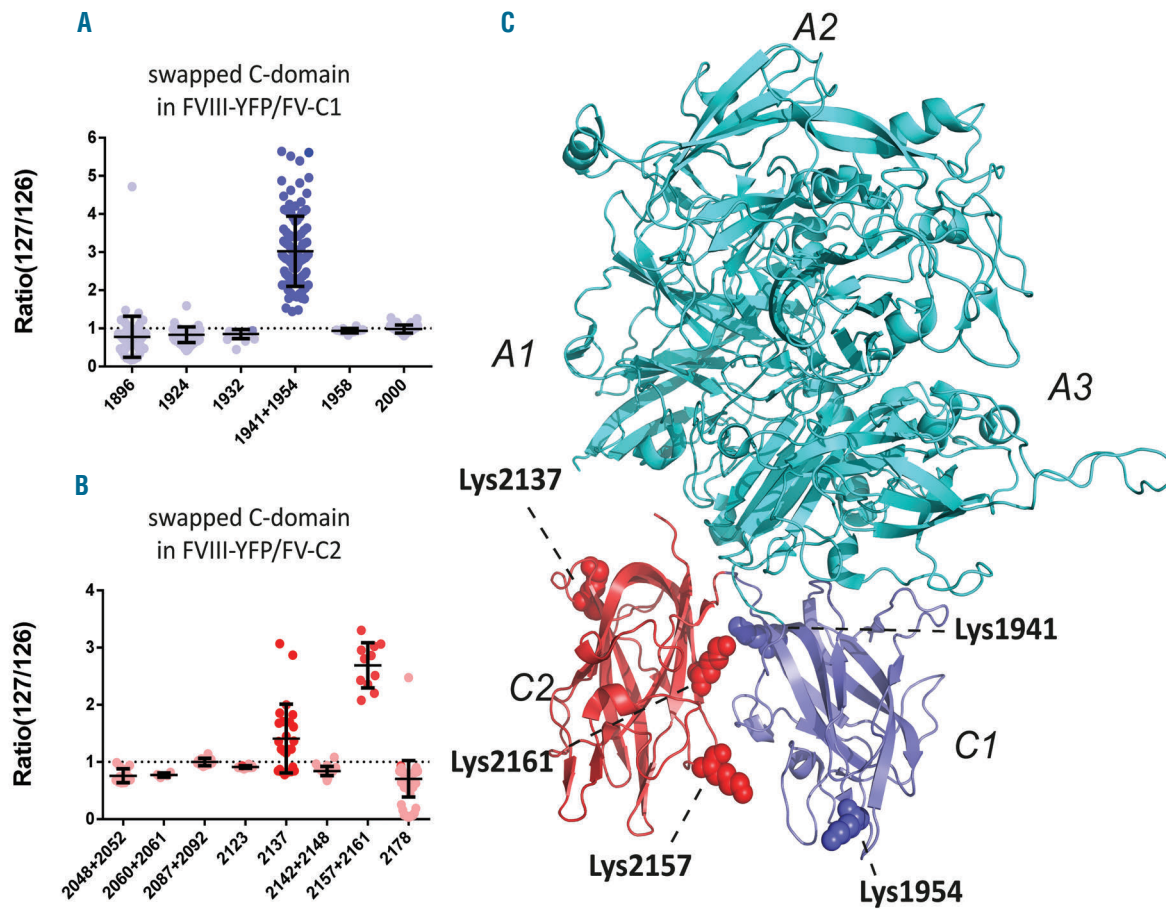


Figure 6. Comparison of FVIII-YFP/FV-C1 and FVIII-YFP/FV-C2 with FV by labeling with tandem-mass tags. FVIII-YFP/FV-C1 and FVIII-YFP/FV-C2 were labeled with TMT-127, and FV with TMT-126. The mean TMT-127/TMT-126 ratio \pm SD (black lines) is given for peptides containing the same lysine residues from (A) the C1-domain in blue and (B) the C2-domain in red of FVIII-YFP/FV-C1 and FVIII-YFP/FV-C2, respectively. Discrete peptides and their measured TMT-127/TMT-126 ratios are represented by dots. Lysine residues with a TMT-127/TMT-126 ratio above 1 (dashed line) are Lys1941+Lys1954, Lys2137 and Lys2157+Lys2161. Such a TMT-127/TMT-126 ratio indicates increased incorporation of TMT-127 and therefore increased accessibility of those lysine residues in the chimera compared to FV wild-type. (C) The lysine residues with TMT-127/TMT-126 ratios above 1 are indicated in a model of FVa (1Y61)³² with spheres. The C1-domain is indicated in blue and the C2-domain in red.

C1-domain associates more tightly with the A3-domain in this chimera, thus maintaining the A3/C1-domain interface undisturbed.

An overall limited disruption of the domain organization is reflected in the activity of the FVIII/FV-C2 chimera. The FVIII/FV-C2 chimera, despite its more accessible C1/C2- and C2/A1-domain interfaces, displays normal FIXa binding and FX activation. Moreover, swapping the entire C2-domain within FVIII does not result in any functional loss (Figure 4B, D). Interestingly, as reported by others, deletion of the C2-domain results in a 4-fold reduction in FIXa affinity.³³ Apparently, the presence of the C1-domain alone is insufficient for full cofactor function. However, the C2-domain of FV fully compensates for this defect (Figure 4B). This apparent paradox can be explained by a complementary role for the C2-domain in its FIXa-binding conformation. Unlike the C2-domain, the C1-domain contributes directly to FIXa binding. This is in agreement with the observation of Wakabayashi *et al.*, who noted that a FVIII variant with the C1-domain replaced by a second C2-domain exhibits an approximately 9-fold reduced affinity for FIXa.³⁴

The FVIII/FV-C1 chimera has a VWF-binding defect that

is more severe than that of FVIII lacking the sulfated tyrosine on position 1680 (FVIII-Y1680F).^{11,12} This is even more prominent at pH 5.5 (Figure 3 and *Online Supplementary Figure S2*) and implies that apart from the sulfated Tyr1680, the FVIII C1-domain is essential for VWF/FVIII complex formation. This is in agreement with previous reports that mutations in the C1-domain can interfere with VWF binding,^{5,12} although this does not exclude an additional contribution of the C2-domain.⁴ A direct C1-domain interaction with VWF is further supported by recent studies using hydrogen-deuterium exchange and electron microscopy,^{35,36}

Previously, we analyzed a variety of FVIII mutations that are associated with reduced interaction with VWF, but normal trafficking to WPB.¹² The fact that these variants retained some residual VWF binding at pH 5.5 led us to speculate that this might be sufficient for trafficking to WPB.¹² In this respect the FVIII/FV-C1 chimera is more defective than the mutations causing hemophilia A which we studied. If FVIII storage with VWF is driven exclusively by VWF binding, this might explain the trafficking defect for FVIII/FV-C1 (Figure 2B). Surprisingly, although the VWF binding of FVIII/FV-C2 is close to normal, this

chimera also displays reduced WPB storage and intracellular accumulation in BOEC (Figure 2C). This supports the conclusion that FVIII trafficking to WPB requires the tandem C-domain pair. This would be compatible with our previous data, because none of the hemophilia A-causing mutations that we analyzed can be expected to disrupt the C-domain pair.¹²

One limitation of lentiviral BOEC transduction is the variability in expression which precludes obtaining quantitative information for direct comparison of the extent of WPB trafficking with VWF-binding affinity. As we showed previously, this issue can be addressed by subcellular fractionation, provided that expression and transduction efficiency are in the same order of magnitude.^{10,12} However, this proved unfeasible for the present set of FVIII/FV chimeras. Nevertheless, it seems evident that the intracellular YFP-staining for the FVIII/FV-C2 chimera, despite its high affinity for VWF, is different from that of FVIII-YFP or BDD-FVIII (Figures 1A and 2A,C). Likewise, the FVIII/FV-C1 chimera, which displays no appreciable VWF interaction, could not be visualized intracellularly (Figure 2B). Despite these trafficking defects in BOEC, the chimeras could be expressed in HEK293 cells, and after purification displayed structural integrity and functionality (Figures 4-6 and Online

Supplementary Figure S3). This might suggest that besides VWF binding another, as yet unknown mechanism could play a role in endothelial FVIII storage and secretion. A role for the A1-domain could not be excluded because the chimeras, compared to FVIII-YFP, display a structural change in the A1-domain as well (Lys47+Lys48, Figure 5). Whether or not these A1-domain residues contribute to maintaining the C-domain tandem organization remains an open question.

Our finding that the C2-domain of FVIII can be replaced by that of FV without compromising FVIII activity may have translational implications. It has been well established that hemophilia A patients with FVIII inhibitors often have antibodies against the C2-domain.³⁷ It seems conceivable that such inhibitors may be bypassed by FVIII containing the FV C2-domain. Because swapping the C1 domain eliminates VWF binding and affects the interaction with FIXa, the potential of FVIII containing the FV C1-domain for bypassing C1-domain-directed inhibitors seems less evident.

Acknowledgments

The authors thank J.M. Koornneef for providing purified factor V. This study was supported by the Landsteiner Foundation for Blood Transfusion Research (LSBR).

References

- Lenting PJ, van Mourik JA, Mertens K. The life cycle of coagulation factor VIII in view of its structure and function. *Blood*. 1998;92(11):3983-3996.
- Thompson AR. Structure and function of the factor VIII gene and protein. *Semin Thromb Hemost*. 2003;29(1):11-22.
- Leyte A, van Schijndel HB, Niehrs C, et al. Sulfation of Tyr1680 of human blood coagulation factor VIII is essential for the interaction of factor VIII with von Willebrand factor. *J Biol Chem*. 1991;266(2):740-746.
- Saenko EL, Scandella D. The acidic region of the factor VIII light chain and the C2 domain together form the high affinity binding site for von Willebrand factor. *J Biol Chem*. 1997;272(29):18007-18014.
- Jacquemin M, Lavend'homme R, Benhida A, et al. A novel cause of mild/moderate hemophilia A: mutations scattered in the factor VIII C1 domain reduce factor VIII binding to von Willebrand factor. *Blood*. 2000;96(3):958-965.
- Fahs SA, Hille MT, Shi Q, Weiler H, Montgomery RR. A conditional knockout mouse model reveals endothelial cells as the principal and possibly exclusive source of plasma factor VIII. *Blood*. 2014;123(24):3706-3713.
- Everett LA, Cleuren AC, Khoriaty RN, Ginsburg D. Murine coagulation factor VIII is synthesized in endothelial cells. *Blood*. 2014;123(24):3697-3705.
- Shahani T, Covens K, Lavend'homme R, et al. Human liver sinusoidal endothelial cells but not hepatocytes contain factor VIII. *J Thromb Haemost*. 2014;12(1):36-42.
- Rosenberg JB, Foster PA, Kaufman RJ, et al. Intracellular trafficking of factor VIII to von Willebrand factor storage granules. *J Clin Invest*. 1998;101(3):613-624.
- Van den Biggelaar M, Bouwens EAM, Kootstra NA, Hebbel RP, Voorberg J, Mertens K. Storage and regulated secretion of factor VIII in blood outgrowth endothelial cells. *Haematologica*. 2009;94(5):670-678.
- Van den Biggelaar M, Bierings R, Storm G, Voorberg J, Mertens K. Requirements for cellular co-trafficking of factor VIII and von Willebrand factor to Weibel-Palade bodies. *J Thromb Haemost*. 2007;5(11):2235-2242.
- Van den Biggelaar M, Bouwens EA, Voorberg J, Mertens K. Storage of factor VIII variants with impaired von Willebrand factor binding in Weibel-Palade bodies in endothelial cells. *PLoS One*. 2011;6(8):e24163.
- Lu J, Pipe SW, Miao H, Jacquemin M, Gilbert GE. A membrane-interactive surface on the factor VIII C1 domain cooperates with the C2 domain for cofactor function. *Blood*. 2011;117(11):3181-3189.
- Gilbert GE, Novakovic VA, Kaufman RJ, Miao H, Pipe SW. Conservative mutations in the C2 domains of factor VIII and factor V alter phospholipid binding and cofactor activity. *Blood*. 2012;120(9):1923-1932.
- Gilbert GE, Kaufman RJ, Arena AA, Miao H, Pipe SW. Four hydrophobic amino acids of the factor VIII C2 domain are constituents of both the membrane-binding and von Willebrand factor-binding motifs. *J Biol Chem*. 2002;277(8):6374-6381.
- Peng W, Quinn-Allen MA, Kane WH. Mutation of hydrophobic residues in the factor Va C1 and C2 domains blocks membrane-dependent prothrombin activation. *J Thromb Haemost*. 2005;3(2):351-354.
- Adams TE, Hockin MF, Mann KG, Everse SJ. The crystal structure of activated protein C-inactivated bovine factor Va: Implications for cofactor function. *Proc Natl Acad Sci USA*. 2004;101(24):8918-8923.
- Bos MH, Camire RM. Blood coagulation factors V and VIII: molecular mechanisms of procofactor activation. *J Coagul Disord*. 2010;2(2):19-27.
- Bos MHA, Meijerman DWE, van der Zwaan C, Mertens K. Does activated protein C-resistant factor V contribute to thrombin generation in hemophilic plasma? *J Thromb Haemost*. 2005;3(3):522-530.
- Meems H, van den Biggelaar M, Rondaj M, van der Zwaan C, Mertens K, Meijer AB. C1 domain residues Lys 2092 and Phe 2093 are of major importance for the endocytic uptake of coagulation factor VIII. *Int J Biochem Cell Biol*. 2011;43(8):1114-1121.
- Bloem E, van den Biggelaar M, Wroblewska A, Voorberg J, et al. Factor VIII C1 domain spikes 2092-2093 and 2158-2159 comprise regions that modulate cofactor function and cellular uptake. *J Biol Chem*. 2013;288(41):29670-29679.
- Bloem E, Ebberink EH, van den Biggelaar M, van der Zwaan C, Mertens K, Meijer AB. A novel chemical footprinting approach identifies critical lysine residues involved in the binding of receptor-associated protein to cluster II of LDL receptor-related protein. *Biochem J*. 2015;468(1):65-72.
- Bouwens EA, Mourik MJ, van den Biggelaar M, et al. Factor VIII alters tubular organization and functional properties of von Willebrand factor stored in Weibel-Palade bodies. *Blood*. 2011;118(22):5947-5956.
- Van den Biggelaar M, Meijer AB, Voorberg J, Mertens K. Intracellular cotrafficking of factor VIII and von Willebrand factor type 2N variants to storage organelles. *Blood*. 2009;113(13):3102-3109.

25. Van den Biggelaar M, Madsen JJ, Faber JH, et al. Factor VIII interacts with the endocytic receptor low-density lipoprotein receptor-related protein 1 via an extended surface comprising "hot-spot" lysine residues. *J Biol Chem.* 2015;290(27):16463-16476.
26. Wu MM, Grabe M, Adams S, Tsien RY, Moore HP, Machen TE. Mechanisms of pH regulation in the regulated secretory pathway. *J Biol Chem.* 2001;276(35):33027-33035.
27. Vogel W. Discoidin domain receptors: structural relations and functional implications. *FASEB J.* 1999;13 (Suppl):S77-82.
28. Véron P, Segura E, Sugano G, Amigorena S, Théry C. Accumulation of MFG-E8/lactadherin on exosomes from immature dendritic cells. *Blood Cells Mol Dis.* 2005;35(2):81-88.
29. Oshima K, Aoki N, Kato T, Kitajima K, Matsuda T. Secretion of a peripheral membrane protein, MFG-E8, as a complex with membrane vesicles. *Eur J Biochem.* 2002;269(4):1209-1218.
30. Shen BW, Spiegel PC, Chang C-H, et al. The tertiary structure and domain organization of coagulation factor VIII. *Blood.* 2008;111(3):1240-1247.
31. Ngo JC, Huang M, Roth DA, Furie BC, Furie B. Crystal structure of human factor VIII: implications for the formation of the factor IXa-factor VIIIa complex. *Structure.* 2008;16(4):597-606.
32. Orban T, Kalafatis M, Gogonea V. Completed three-dimensional model of human coagulation factor vs. molecular dynamics simulations and structural analyses. *Biochemistry.* 2005;44(39):13082-13090.
33. Wakabayashi H, Griffiths AE, Fay PJ. Factor VIII lacking the C2 domain retains cofactor activity *in vitro*. *J Biol Chem.* 2010;285(33):25176-25184.
34. Wakabayashi H, Fay PJ. Replacing the factor VIII C1 domain with a second C2 domain reduces factor VIII stability and affinity for factor IXa. *J Biol Chem.* 2013;288(43):31289-31297.
35. Chiu PL, Bou-Assaf GM, Chhabra ES, et al. Mapping the interaction between factor VIII and von Willebrand factor by electron microscopy and mass spectrometry. *Blood.* 2015;126(8):935-938.
36. Yee A, Oleskie AN, Dosey AM, et al. Visualization of an N-terminal fragment of von Willebrand factor in complex with factor VIII. *Blood.* 2015;126(8):939-942.
37. Meeks SL, Healey JF, Parker ET, Barrow RT, Lollar P. Antihuman factor VIII C2 domain antibodies in hemophilia A mice recognize a functionally complex continuous spectrum of epitopes dominated by inhibitors of factor VIII activation. *Blood.* 2007;110(13):4234-4242.